JOURNAL OF MATERIALS SCIENCE 11 (1976) 291–296

The elastic constants of antimony-25.5 at. % arsenic alloy single crystals

Y. C. AKGÖZ*, C. ISCI, G. A. SAUNDERS†
Department of Applied Physics and Electronics, University of Durham, Science Laboratories, South Road, Durham, UK

The six independent elastic constants of single crystals of the homogeneous, minimum melting point alloy of composition antimony 74.5 at. % and arsenic 25.5 at. % have been measured. The elastic behaviour of the alloy is compared with that of the rhombohedral A7 structure elements arsenic and antimony and is found to show characteristics consistent with those expected for layer-type crystals. Elastic wave velocity surface cross-sections, particle displacement and energy flux vectors and Young's modulus are presented and discussed. The Debye temperature is 219 K.

1. Introduction

The elastic properties of alloys can be markedly affected by the presence of inhomogeneities. The aim of the present work has been to measure the elastic constants of a binary alloy of high perfection and compare the results with those of the parent elements. Usually for solid solution systems the solidus and liquidus are separated on the phase diagram and, in consequence, extensive constitutional supercooling can onset in the liquid alloy near a freezing interface and solute segregation in the frozen material can result. However, in the antimony–arsenic solid solution system there is a minimum melting point at which the solidus and liquidus touch [1–4]: the liquid and solid phase in equilibrium have the same composition (25.5 at. % As) [1]. Crystals grown with this composition are homogeneous and of high perfection [5] and so are well suited to the present purpose. The elastic constants of this alloy have been measured by ultrasonic techniques and the results are compared with those of the parent elements arsenic and antimony.

2. Experimental procedure

Single crystals of the minimum melting temperature (612° C) antimony–25.5 at. % arsenic alloy were grown from 99.9999% purity elements by a modified Bridgman technique. A detailed description of the crystal growth and of an examination of perfection have been given in [5]. The crystals showed no cellular or dendritic structure or other growth inhomogeneities. Electron microprobe analysis showed that the composition was constant along the crystal length to within the experimental error (± 0.5% composition change) of the probe. Etch pit studies on (1 1 1) cleavage plane faces have shown that the dislocation densities are particularly low (10^3 cm^{-2}) for an alloy. The primitive lattice parameter a is equal to 4.418 ± 0.001 Å and the rhombohedral angle α is 56° 12′ ± 3′. This alloy is semimetallic having equal electron and hole densities of 6.2×10^{25} m^{-3} at 77 K (1.6 and 0.32 times those of antimony and arsenic respectively); carrier mobilities, being dominated by alloy scattering, are much smaller than those of the parent elements; at low temperatures the carrier mobility is constant and above 60 K varies as $T^{-0.4}$ [6].

The arsenic–antimony alloys have the A7 crystal structure (point group $\bar{3}m$). The sign of the elastic constant C_{14} depends upon the definition of the crystallographic reference frame with respect to the atomic arrangement in the particular crystal being studied [7–11]. The convention used here for definition of an unambiguous right handed

*Present address: Physics Department, Middle East Technical University, Ankara, Turkey.
† Present address: School of Physics, University of Bath, Claverton Down, Bath, UK.

$(+x, +y, +z)$ axial set is that described in detail elsewhere [7–13], suffice to say that a $(+x, +y, +z)$ axial set has been assigned to the crystal by use of Laue back-reflection photographs and that in the convention used the $+y+z$ quadrant in the mirror plane contains a pseudo-three-fold axis and the $-y+z$ quadrant a pseudo-four-fold axis. Crystals used for the ultrasound wave velocity measurements were aligned to within $+\frac{1}{2}°$ of the prerequisite crystallographic direction and then spark-cut and planed to have flat and parallel faces to within 0.0001 cm. Ultrasonic wave transit times were measured to an accuracy of $\pm 0.001\%$ by the pulse echo overlap technique [14] at a carrier frequency of 10 Mhz. To excite and receive the ultrasound waves, gold-plated quartz transducers were used bonded with Nonaq. The velocity measurements are accurate to $\pm 0.8\%$ – the sum of uncertainties due to misorientation ($< 0.4\%$), diffraction loss ($< 0.1\%$), uncertainty in the transit time due to phase change on reflection at the specimen–bond–transducer interface ($< 0.2\%$) and in measurement of sample length ($< 0.03\%$).

3. Ultrasonic wave propagation in the alloy single crystals

In a specified crystallographic direction, defined by direction cosines n_1, n_2, n_3, three bulk elastic waves can be propagated with velocities and polarizations determined by the eigenvalues and

TABLE I The relationships between the elastic stiffness constants and the experimental ultrasound velocities at room temperature in Sb–25.5 at. % As alloy single crystals.

Relations	Wave-vector direction	Polarization vector	Experimental velocity ($\times 10^5$ cm sec^{-1})
$\rho v_1^2 = C_{11}$	$\begin{bmatrix}1\\0\\0\end{bmatrix}$	$\begin{bmatrix}1\\0\\0\end{bmatrix}$	4.017
$\rho v_2^2 = \frac{1}{2}[(C_{66}+C_{44}) + ((C_{44}-C_{66})^2 + 4C_{14}^2)^{1/2}]$		$\begin{bmatrix}0\\0.9903\\-0.1392\end{bmatrix}$	2.952
$\rho v_3^2 = \frac{1}{2}\{(C_{66}+C_{44}) - [(C_{44}-C_{66})^2 + 4C_{14}^2]^{1/2}\}$		$\begin{bmatrix}0\\0.1392\\0.9903\end{bmatrix}$	1.483
$\rho v_4^2 = C_{33}$	$\begin{bmatrix}0\\0\\1\end{bmatrix}$	$\begin{bmatrix}0\\0\\1\end{bmatrix}$	2.678
$\rho v_5^2 = C_{44}$		[in xy plane]	2.480
$\rho v_6^2 = \frac{1}{2}(C_{11}+C_{33}) + C_{44} - C_{14} + [(\frac{1}{2}C_{11} - C_{33} - C_{14})^2 + (C_{13}+C_{44}-C_{14})^2]^{1/2}$	$\begin{bmatrix}0\\\frac{1}{\sqrt{2}}\\\frac{1}{\sqrt{2}}\end{bmatrix}$	$\begin{bmatrix}0\\0.7821\\0.6231\end{bmatrix}$	3.290
$\rho v_7^2 = \frac{1}{2}(C_{11}+C_{33}) + C_{44} - C_{14} - [(\frac{1}{2}C_{11} - C_{33} - C_{14})^2 + (C_{13}+C_{44}-C_{14})^2]^{1/2}$		$\begin{bmatrix}0\\0.6231\\-0.7821\end{bmatrix}$	1.860
$\rho v_8^2 = \frac{1}{2}(C_{66}+C_{44}) + C_{14}$		$\begin{bmatrix}1\\0\\0\end{bmatrix}$	2.672

Density is 6.560 g cm^{-3}.

eigenvectors of the Christoffel equations

$$(L_{ik} - \rho v^2 \delta_{ik}) u_{0k} = 0 \quad (i = 1, 2, 3) \quad (1)$$

u_{01}, u_{02}, u_{03} are the direction cosines of the particle displacement vectors and the Christoffel coefficients L_{ik} for the RI Laue group (point groups 32, $3m$, $\bar{3}m$) are

$$\begin{aligned}
L_{11} &= n_1^2 C_{11} + n_2^2 C_{66} + n_3^2 C_{44} + 2n_2 n_3 C_{14} \\
L_{22} &= n_1^2 C_{66} + n_2^2 C_{11} + n_3^2 C_{44} - 2n_2 n_3 C_{14} \\
L_{33} &= (n_1^2 + n_2^2) C_{44} + n_3^2 C_{33} \\
L_{12} &= 2n_1 n_3 C_{14} + \tfrac{1}{2} n_1 n_2 (C_{11} + C_{12}) \\
L_{13} &= n_1 n_3 (C_{44} + C_{13}) + 2n_1 n_2 C_{14} \\
L_{23} &= (n_1^2 - n_2^2) C_{14} + n_2 n_3 (C_{13} + C_{44}).
\end{aligned} \quad (2)$$

The three eigenvalues of the determinantal Equation 1 define, in terms of the elastic stiffness constants C_{ij} and the propagation direction n_i, the velocities of the three orthogonal modes. The polarization of a mode is obtained by substituting its velocity back into Equation 1 and solving for u_{0k}. The relationships between the velocity and the elastic constants for the selected propagation directions are given in Table I, together with the polarization directions and the measured velocities. The elastic constants calculated from these data by a least-mean-squares procedure are compared with those of the parent elements in Table II. Arsenic differs from the other two V elements of A7 structure antimony and bismuth in that C_{14} has a negative and S_{14} ($= -1/C_{14}$) a positive sign [7–10]. The significance of this difference is best seen by considering the effect of a tensile stress σ_{11} applied along the x-axis; the resultant strains are $\epsilon_{11} = S_{11}\sigma_{11}$; $\epsilon_{22} = S_{12}\sigma_{11}$; $\epsilon_{33} = S_{13}\sigma_{11}$; $\epsilon_{32} = \epsilon_{23} = S_{14}\sigma_{11}$. Thus the sense of the associated shear ϵ_{32} for arsenic is different from that of antimony or bismuth. For the arsenic–antimony alloy C_{14} and S_{14} have the same signs as for antimony.

Knowledge of the complete set of elastic constant tensor components allows determination of the material response to an applied stress system. The surface showing the variation of Young's modulus Y with direction l of an applied tensile stress is a useful aid to visualization of a material's elastic anisotropy. For a crystal belonging to one of the point groups 32, $\bar{3}m$ or $3m$ is given by

$$\begin{aligned}
Y^{-1} &= (1 - l_3^2)^2 S_{11} + l_3^4 S_{33} \\
&\quad + l_3^2 (1 - l_3^2)(2S_{13} + S_{44}) \\
&\quad + 2l_2 l_3 (3l_1^2 - l_2^2) S_{14}.
\end{aligned} \quad (3)$$

TABLE II

	Arsenic [10]	Antimony [8]	As (25.5 At.%)–Sb
Elastic stiffness ($\times 10^{10}$ dyn cm^{-2})			
C_{11}	130.2 ± 1.0	99.4	105.5 ± 1.2
C_{12}	30.3 ± 2.1	30.9	45.4 ± 3.0
C_{13}	64.3 ± 1.1	26.4	27.7 ± 0.8
C_{14}	−3.71 ± 0.52	21.6	17.6 ± 1.2
C_{33}	58.7 ± 1.0	44.5	47.2 ± 0.8
C_{44}	22.5 ± 0.5	39.5	40.3 ± 0.5
C_{66}	50.0 ± 1.6	34.2	30.1 ± 2.0
Elastic compliance constants ($\times 10^{-13}$ cm^2 dyn^{-1})			
S_{11}	30.3	16.2	15.40
S_{12}	20.2	−6.1	−6.96
S_{13}	−55.2	−5.9	−4.96
S_{14}	1.67	−12.2	−9.76
S_{33}	137.8	29.5	27.00
S_{44}	45.0	38.6	33.34
S_{66}	20.2	44.6	44.72
Linear comp., β_t, 10^{-13} cm^2 dyn^{-1}	−4.9	4.1	3.5
Linear comp., β_z, 10^{-13} cm^2 dyn^{-1}	27.6	17.5	17.1
Volume comp., β_v, 10^{-13} cm^2 dyn^{-1}	18.0	25.8	24.1
Debye temp., θ_D (K)	227	209	219
Long. mode, θ_L (K)	460	342	362
Shear mode, θ_{T_1} (K)	271	230	235
Shear mode, θ_{T_2} (slow) (K)	172	165	175

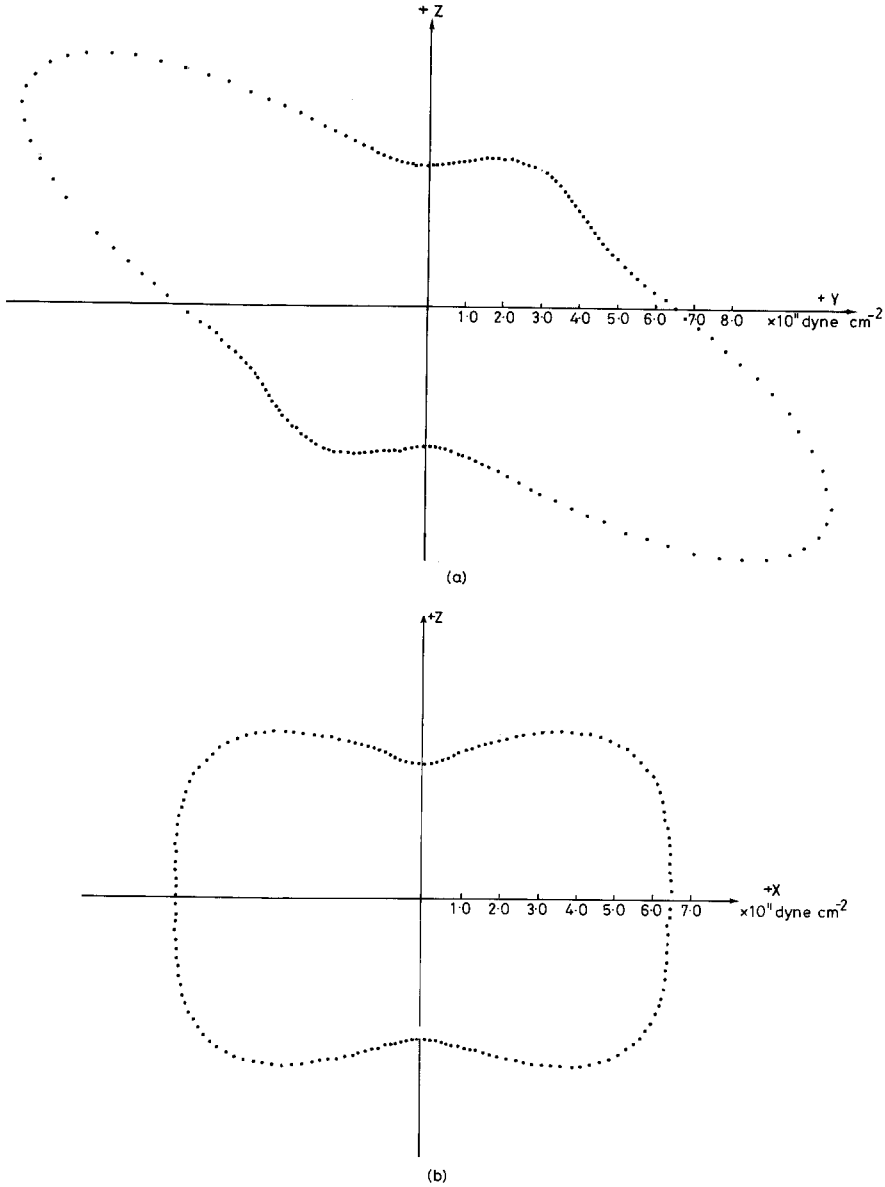

Figure 1 The (a) *yz* and (b) *xz* cross-sections of the Young's modulus surface for monocrystalline antimony – 25.5 at.% arsenic alloy.

The (*yz*, *xz*) cross-sections of the Young's modulus surface of the alloy are plotted in Fig. 1; they are similar to those of antimony [15]. The directional dependence of the Young's modulus reflects the layer-like nature of the alloy.

By computation of the eigenvalues of the Christoffel Equation 1, the three wave velocities have been obtained for wave propagation at 2° intervals around the *xy*, *yz* and *xz* planes (Fig. 2). Arsenic, and to a lesser extent antimony, is a layer-like crystal with strong interatomic binding forces within each double layer (parallel to the *xy* plane) but binding between successive double layers (stacked along the *z*-direction) is relatively weak; the elastic behaviour reflects this layer structure [9, 10]. On the evidence of its ready cleavage to expose (1 1 1) faces [5, 13], the alloy also shows a layer-like nature, the phase velocity surfaces add confirmation to this suggestion. Both the *yz* and *xz* plane cross-sections are compressed (although not to the same extent as those in arsenic) along the *z*-direction, a manifestation of weaker binding along the *z*-axis than in the *xy* plane; in a layer structure velocities of elastic wave transmitted within the tightly bound layers are greater than those of waves propagated along the direction of

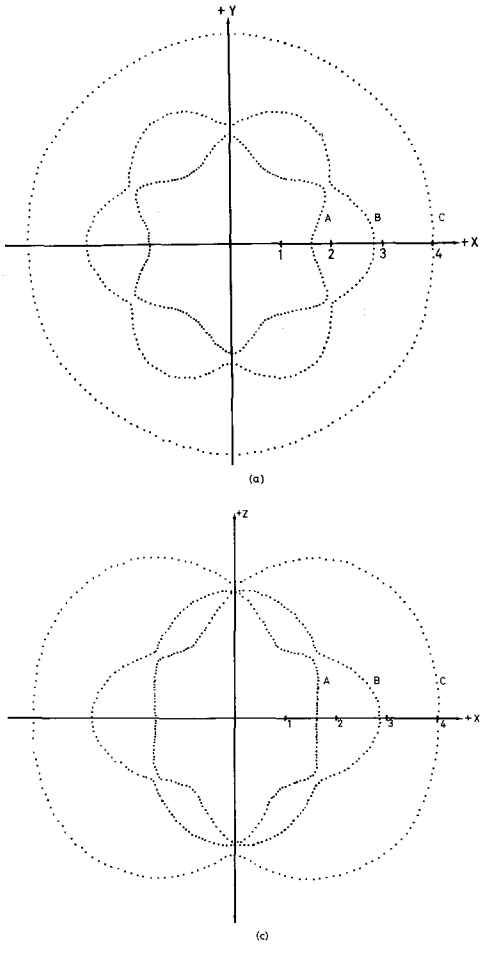

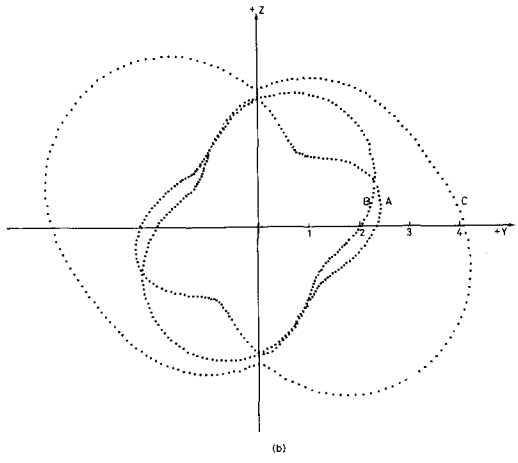

Figure 2 The (a) xy, (b) yz and (c) xz cross-sections of the velocity surfaces of antimony – 25.5 at. % arsenic alloy; A and B refer to the slow and fast quasi-shear waves respectively and C to the quasi-longitudinal wave. Units are 10^5 cm sec^{-1}.

weak binding.

For $\bar{3}m$ crystals ultrasonic wave transmission in the yz mirror plane is a special case: one pure shear wave with $\boldsymbol{u}$ parallel to the binary (x) axis can be propagated along any direction in this plane (with a velocity given by $[(n_2^2(C_{66} - C_{44}) + C_{44} + 2n_2n_3C_{14})/\rho]^{1/2}$. Therefore, orthogonality demands that the other two waves have polarization vectors lying in the yx plane; these polarization vectors have been calculated as the eigenvectors of Equation 1; the deviation of the polarization vector from the propagation direction for one wave, which has predominantly longitudinal character, is plotted in Fig. 3. Not only is the condition $\boldsymbol{u} \times \boldsymbol{n} = 0$ for pure longitudinal mode propagation obeyed along the z-axis, but also for the direction at 154° to the $+y$ axis in the yz plane. By orthogonality the third mode must be pure transverse and, therefore, this

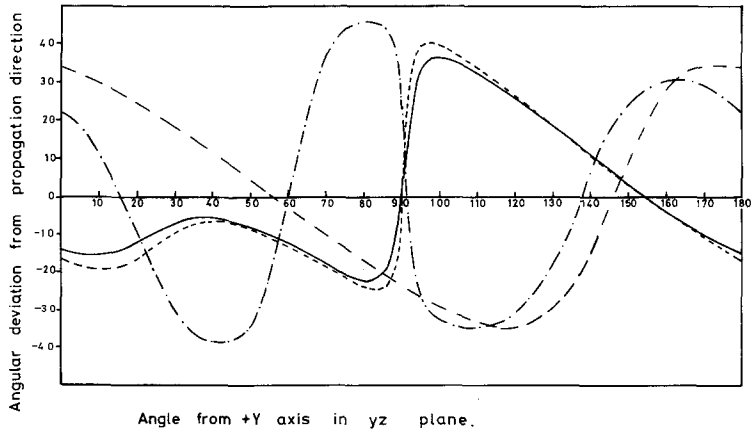

Figure 3 The deviations from propagation directions in the yz plane of antimony – 25.5 at. % arsenic alloy: (i) the particle displacement associated with the quasi-longitudinal wave (————), (ii) the energy flux associated with the quasi-longitudinal wave (— — — — —), (iii) the energy flux associated with the quasi-shear wave (—·—·—·) and (iv) the energy flux associated with pure shear (—— —— ——).

direction is an accidental pure mode direction: knowledge of the existence of such directions is most useful in ultrasonic studies. The energy flux vector for modes propagated in the yz plane has been calculated from [10]:

$$P_i = -\sigma_{ij}\dot{u}_j = \frac{-(pw)^2}{2v} C_{ijkl}u_{0j}u_{0k}u_{0l}n_1$$

Results are also plotted in Fig. 3. For $\bar{3}m$ crystals, the energy flux component P_1 along the x-axis is zero for all three modes propagating in the yz plane: the energy flow is always in the yz plane for any mode propagating in any direction in that plane. Although the energy flux associated with a pure mode (longitudinal) is always parallel to the propagation direction, this is not so for a pure transverse mode, unless the mode axis has two-fold, four-fold, or six-fold rotational symmetry or is normal to a plane of reflection symmetry [16]. For the accidental pure transverse mode in the alloy the energy flux deviates by $+28°$ from the pure mode axis, while that for the pure transverse mode is $+20°$.

The elastic constant data have been used to calculate the Debye temperature θ_D from

$$\theta_D = \left(\frac{9N}{4\pi}\right)^{1/3} \frac{h}{k} \Bigg/ \left(\int \left[\frac{1}{v_1^3} + \frac{1}{v_2^3} + \frac{1}{v_3^3}\right] \frac{d\Omega}{4\pi}\right)^{1/3}.$$

Here the v_i are the eigenvalues. The integral over solid angle $d\Omega$ must be taken over all directions and has been approximated by a sum taken at 10288 points each subtending an equal solid angle $\Delta\Omega$ (1.218×10^{-3} steradians). The same procedure was used to calculate the Debye temperature θ_i appropriate to each mode using

$$\theta_i = \left(\frac{3N}{4\pi}\right)^{1/3} \frac{h}{k} \Bigg/ \left(\int \left[\frac{1}{v_i^3}\right] \frac{d\Omega}{4\pi}\right)^{1/3}$$

The calculated Debye temperatures for arsenic, antimony and the alloy are given in Table II.

The volume and linear compressibilities of the alloy are compared with those of the parent elements in Table II. Under hydrostatic pressure the linear change along the z-direction is 4.9 larger than that in the xy plane – direct evidence of the layer-like structure: the compressibilities depend upon the second derivative of the lattice potential energy. It has been proposed [17] that the bulk modulus of a homogeneous solid solution alloy could be approximately the arithmetic mean of the bulk moduli of the constituents, if the energy of phase formation is not strongly volume dependent. This is not so for this alloy: the bulk modulus (the inverse of the volume compressibility, Table II) is identical within experimental error to that of antimony. In general the elastic behaviour of the alloy resembles that of antimony much more than that of arsenic.

References

1. N. PARRAVANO and P. DE CESARIS, *Z. Metallk.* **2** (1912) 70.
2. Q. A. MANSURI, *J. Chem. Soc.* **2** (1928) 2107.
3. C. H. SHIH and E. A. PERETTI, *Amer. Soc. Metals Trans.* **48** (1956) 706.
4. B. J. SKINNER, *Econ. Geol.* **60** (1965) 228.
5. Y. C. AKGÖZ and G. A. SAUNDERS, *J. Mater. Sci.* **6** (1971) 395.
6. *Idem, J. Phys. C* 7 (1974) 1655.
7. Y. ECKSTEIN, A. W. LAWSON and D. H. RENEKER, *J. Appl. Phys.* **31** (1960) 1535.
8. S. EPSTEIN and A. P. DE BRETTEVILLE, *Phys. Rev.* **138** (1965) A771.
9. N. G. PACE, G. A. SAUNDERS and Z. SÜMENGEN, *J. Phys. Chem. Solids* **31** (1970) 1467.
10. N. G. PACE and G. A. SAUNDERS, *ibid* **32** (1971) 1585.
11. Y. C. AKGÖZ, G. A. SAUNDERS and Z. SÜMENGEN, *J. Mater. Sci.* **7** (1972) 279.
12. R. D. BROWN, R. L. HARTMAN and S. H. KOENIG, *Phys. Rev.* **172** (1968) 598.
13. Y. C. AKGÖZ, J. M. FARLEY and G. A. SAUNDERS, *J. Mater. Sci.* 7 (1972) 598.
14. E. P. PAPADAKIS, *J. Acoust. Soc. Amer.* **42** (1967) 1045.
15. D. J. GUNTON and G. A. SAUNDERS, *J. Mater. Sci.* 7 (1972) 1061.
16. P. C. WATERMAN, *Phys. Rev.* **113** (1959) 1240.
17. J. F. SMITH, "Nuclear Metallurgy" Vol. **10,** edited by J. T. Waber, P. Chiotti and W. N. Miner (Edwards, Ann Arbor, Michigan, 1964) p. 397.

Received 10 June and accepted 27 July 1975.